5-Diisopropoxyphosphoryl-5-methyl-1-pyrroline *N*-oxide, DIPPMPO, a crystalline analog of the nitrone DEPMPO: synthesis and spin trapping properties †

Florence Chalier * and Paul Tordo

Laboratoire "Structure et Réactivité des Espèces Paramagnétiques", UMR 6517, CNRS et Universités d'Aix-Marseille I et III, Faculté de Saint Jérôme, case 521, 13397 Marseille Cedex 20, France. E-mail: chalier@srepir1.univ-mrs.fr; Fax: (33) 4 91 28 85 12; Tel: (33) 4 91 28 85 62

Received (in Cambridge, UK) 15th July 2002, Accepted 10th October 2002
First published as an Advance Article on the web 12th November 2002

The nitrone DIPPMPO (5-diisopropoxyphosphoryl-5-methyl-1-pyrroline *N*-oxide) was synthesised, isolated as hygroscopic crystals and its X-ray geometry was determined. The purification of DIPPMPO was easy, compared with that of DEPMPO (5-diethoxyphosphoryl-5-methyl-1-pyrroline *N*-oxide) and its solutions in phosphate buffer were EPR silent. DIPPMPO exhibits all the advantages of DEPMPO for the spin-trapping of biological free radicals and thus DIPPMPO is a choice tool in this field.

Introduction

Of all the techniques used to study free radicals in biological cells and tissues, none is more direct and definitive than electron paramagnetic resonance spectroscopy (EPR).[1] Nevertheless for the detection of many important biological free radicals with very short life times, spin trapping techniques have been associated with EPR.[2] In order to investigate free radical processes in biological milieus, an efficient spin trap[3] should fulfil several criteria. The rate of trapping of the targeted radicals must be fast enough to prevent them from being distracted towards other biological processes,[4] and the resulting spin adducts must be persistent enough to reach and maintain an EPR-detectable concentration. EPR spectra of spin adducts must be easy to assign and they should provide information on the nature of the trapped radicals. To avoid false interpretation, the heterolytic formation of impostor spin adducts[5,6] or the fast decay of the spin adducts to other paramagnetic species[7] must be very minor events. Nitrones have been used to trap various radicals including oxygen centred radicals such as superoxide, $O_2^{-\bullet}$, and the hydroxyl radical, $HO^{\bullet}$. Studies performed in our laboratory clearly showed that, compared with the very popular nitrone DPMO,[8] the phosphorylated nitrone DEPMPO[9] (Scheme 1) presents three major advantages. The first marked

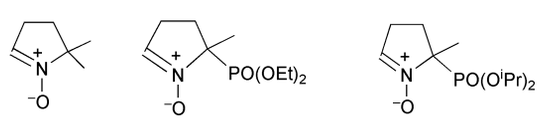

Scheme 1

advantage is the higher persistency of oxygen centred radical adducts and especially that of the superoxide radical (15 times higher) and the alkylperoxyl radicals.[10] Moreover, spontaneous decomposition of the superoxide adduct into the hydroxyl adduct was not observed. The third advantage is the additional information obtained from the phosphorus-coupling constant allowing an easier identification of the trapped radical structure.

Starting from 2-methylpyrroline, DEPMPO can be easily prepared in a two step synthesis.[11] However, DEPMPO is a liquid that decomposes on heating, thus its purification is not straightforward and needs specific equipment and the know-how of an experienced organic chemist. Owing to these difficulties, to obtain highly purified samples of DEPMPO is not a routine task and we decided to search for an analogue of DEPMPO, with the same spin trapping advantages and easier to purify. Stolze *et al.*[12] have investigated a series of DEPMPO analogues bearing various dialkylphosphoryl groups (–P(O)-$(OR)_2$) with n-propoxyl, butoxyl and 2-ethylhexyloxyl substituents. However none of these analogues exhibited advantages comparable with those of the parent DEPMPO. We describe hereafter the synthesis and the spin trapping potentialities of 5-diisopropoxyphosphoryl-5-methyl-1-pyrroline *N*-oxide DIPPMPO (Scheme 1), which has bulkier alkoxyl substituents on phosphorus that could facilitate its crystallisation and confer more lipophilic properties.

Results and discussion

Synthesis

DIPPMPO was easily prepared in a two-step synthesis as shown in Scheme 2. The diisopropyl (2-methyl-2-pyrrolidinyl)-phosphonate **1** was obtained through addition at room tem-

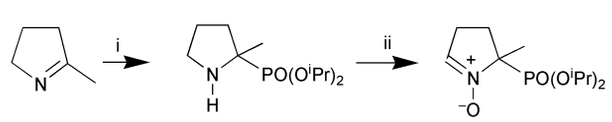

Scheme 2 DIPPMPO synthesis (i) 1.1 eq. $HP(O)(O^iPr)_2$, 20 °C; (ii) 2.2 eq. H_2O_2, 0.04 eq. $WO_4Na_2{\cdot}2H_2O$.

perature of diisopropylphosphite to the commercially available 2-methylpyrroline. Oxidation of crude **1** with H_2O_2, in the presence of a catalytic amount of sodium tungstate led to the crude nitrone DIPPMPO which was then crystallised at −18 °C in a dry and inert atmosphere, and recrystallised in a mixture of pentane and toluene (90/10).

† Electronic supplementary information (ESI) available: Tables of crystallographic data. See http://www.rsc.org/suppdata/p2/b2/b206909c/

 DOI: 10.1039/b206909c

Table 1 X-ray data of DIPPMPO structure

Selected bond lengths of DIPPMPO/Å (with estimated standard deviations in parentheses)

P(1)–O(2)	1.4594(14)	P(1)–O(3)	1.5774(14)	P(1)–O(4)	1.5701(13)	P(1)–C(9)	1.8294(18)
O(3)–C(13)	1.457(2)	O(4)–C(17)	1.472(3)	O(6)–N(5)	1.300(2)	N(5)–C(7)	1.283(3)
N(5)–C(9)	1.499(2)	C(7)–C(11)	1.467(3)	C(8)–C(9)	1.518(3)	C(9)–C(13)	1.542(3)
C(11)–C(13)	1.524(3)	C(14)–C(15)	1.496(5)	C(17)–C(18)	1.504(4)		

Selected angles of DIPPMPO/° (with estimated standard deviations in parentheses)

O(3)P(1)C(9)N(5)	−172.45(12)	O(4)P(1)C(9)N(5)	81.59(13)	O(6)N(5)C(9)P(1)	−65.51(2)
C(7)N(5)C(9)P(1)	112.72(17)	C(7)N(5)C(9)C(13)	−4.59(2)	N(5)C(7)C(11)C(13)	3.19(3)
N(5)C(9)C(13)C(11)	6.13(2)	O(6)N(5)C(7)C(11)	179.00(2)		

X-ray structure

The X-ray data for the DIPPMPO crystals are reported in Table 1, and two DIPPMPO structure views are shown in Fig. 1. The pyrrolinic cycle adopts an E_4 envelop conformation with a small amplitude of the C(11) puckering as shown by the small dihedral angles C(7)N(5)C(9)C(13) (= −4.59°). The C–P bond is in a pseudo-axial geometry with a dihedral angle C(7)-N(5)C(9)P(1) of 112.72°. Examination of Fig. 1 shows that the diisopropoxyphosphoryl group position induces a bigger steric hindrance of the nitrone face where it stands, although the isopropoxyl substituents are oriented towards the exterior of the ring. This steric hindrance that favours *trans* radical addition to the phosphoryl group should be particularly important in water because of solvation.

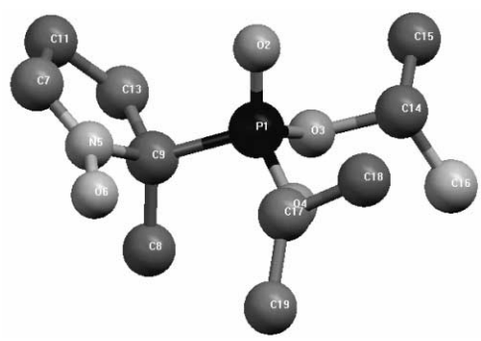

Fig. 1 A perspective of DIPPMPO X-ray structure.

Partition coefficient of DIPPMPO

As a high lipophilicity of the trap could improve its biodistribution in subcellular compartments, we measured the DIPPMPO partition coefficient, K_p, in an octanol–aqueous solution. The K_p value was 2.1 for an octanol–water system while it was 1.24 for an octanol–0.1 M phosphate buffer mixture. For DMPO[13] and DEPMPO[9] in octanol–water the K_p values were reported to be 0.1 and 0.06 respectively. DIPPMPO is thus significantly more lipophilic than DMPO or DEPMPO, and it should be more suitable for trapping experiments conducted in subcellular compartments or lipid rich environments.

Spin trapping experiments

Formation of the superoxide adduct, DIPPMPO/˙OOH. In several physiological disorders it is often proposed that the superoxide radical is the primary upstream radical of the radical reaction chain inducing oxidative stress.[14] Therefore, it was of interest to examine the results of superoxide trapping with DIPPMPO. Superoxide was generated in phosphate buffer (pH = 7.0, 5.6 and 8.2) containing DETAPAC, using the well known (xanthine oxidase–oxygen–hypoxanthine, XO–O_2–HX) system. In the presence of DIPPMPO, whatever the pH value, an intense signal was observed (Fig. 2a). Unambiguous assignment of the signal to the superoxide adduct DIPPMPO/˙OOH was supported by its close similarity to that of DEPMPO/˙OOH, its complete inhibition by the addition of superoxide dismutase (SOD) and its replacement by the signal of DIPPMPO/˙OH in the presence of glutathion peroxidase (30 u cm^{-3}) with 0.03 mM of reduced glutathion.

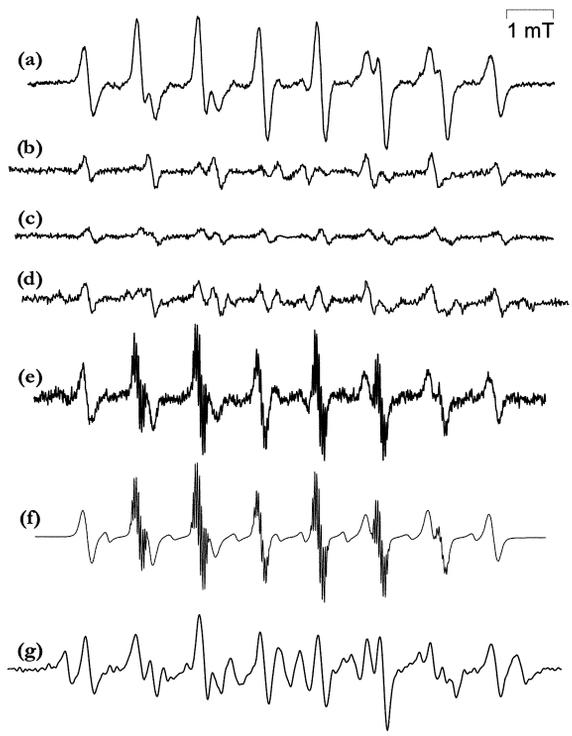

Fig. 2 Observed EPR spectra (a) 1 min after superoxide radical generation by 0.04 u cm^{-3} XO and 0.4 mM HX in 0.1 M phosphate buffer at pH 7 containing 0.02 M DIPPMPO and 1 mM DETAPAC; (b) as for (a) but after 2 h incubation; (c) as for (b) but in the presence of catalase; (d) as for (b) but in the presence of 10% MeOH; (e) as for (a) but 0.05 M DIPPMPO was used under argon atmosphere (f) simulation of the (e) spectrum; (g) after superoxide radical generation by 1 min photolysis of a solution of 0.5 mM riboflavine and 1 mM DETAPAC in 0.1 M phosphate buffer containing also 0.1 M DIPPMPO. Spectrometer settings: microwave power, 10 mW; modulation amplitude, 0.08 mT except for e (0.005); time constant, 0.04 s; gain, 6.3 × 10^5 except for e (4 × 10^5); scan range, 15 mT; scan time, 84 s except for e (672 s).

The intensity of the DIPPMPO/˙OOH signal was dependent on the concentration of xanthine oxidase. At pH 5.6 with a concentration of 0.4 u cm^{-3}, the intensity increased slowly and reached a maximum after 30 min. A ten-fold decrease in the enzyme concentration resulted in a rapid increase of the signal intensity which could still be detected for up to 1 h after generation. This trend suggests that DIPPMPO/˙OOH, like other nitroxides,[7b] can react with superoxide to yield EPR silent products. Signals of comparable intensity were observed when superoxide was trapped, in the same conditions, with either DEPMPO or DIPPMPO. Occasionally, during the decay of the DIPPMPO/˙OOH the hydroxyl adduct signal became detect-

Table 2 EPR parameters of several DIPPMPO radical adducts

DIPPMPO/R$^{\bullet}$	Generating system	Diastereo-isomer	Conformer	A_P/mT	A_N/mT	A_{H_β}/mT	A_{H_γ}/mT
DIPPMPO/$^{\bullet-}O_2$	HX/XO system or riboflavine/UV in 0.1 M buffer	*trans* 90%	T1 (43%)	5.102	1.293	1.234	(1H) 0.088
			T2 (57%)	4.913	1.328	1.023	(1H) 0.089
		*cis*10%		4.209	1.383	0.903	
DIPPMPO/$^{\bullet}OOCH_3$	H_2O_2/UV/O_2 + DMSO 5% in 0.1 M buffer	*trans*	T1 (50%)	5.023	1.321	1.166	
			T2 (50%)	4.743	1.329	0.916	
DIPPMPO/$^{\bullet}OH$	Fenton reaction or H_2O_2/UV in 0.1 M buffer	*trans* 84%		4.688	1.401	1.317	
		cis 16%		3.626	1.596	1.249	
DIPPMPO/$^{\bullet}OMe$	$Pb(OAc)_4$ or MeONa in MeOH			4.671	1.298	0.679	
	10% MeOH in 0.1 M buffer	*trans* 66%		4.756	1.355	0.956	
		cis 34%		3.951	1.375	0.828	
DIPPMPO/$^{\bullet}O^tBu$	^{t}BuO^{t}Bu or ^{t}BuONa in ^{t}BuOH			4.671	1.298	0.679	
	10% ^{t}BuOH in 0.1 M buffer	*trans*		4.646	1.390	1.458	
DIPPMPO/$^{\bullet}CH_3$	Fenton + 200 mM DMSO in 0.1 M buffer	1 species		4.716	1.523	2.261	
		or *trans*	39%	4.769	1.525	2.256	
		cis	61%	4.684	1.522	2.262	
DIPPMPO/$^{\bullet}CH_2OH$	Fenton + 10% MeOH in 0.1 M buffer	1 species		4.904	1.471	2.125	
		or *trans*	41%	4.956	1.474	2.123	
		cis	59%	4.869	1.469	2.126	
DIPPMPO/$^{\bullet}CH(OH)Me$	Fenton + 10% EtOH in 0.1 M buffer	1 species		4.877	1.466	2.149	
		or *trans*	47%	4.933	1.467	2.143	
		cis	53%	4.828	1.464	2.155	
DIPPMPO/$^{\bullet}COOK$	Fenton + 10% HCOOK in 0.1 M buffer	*trans*		4.934	1.440	1.711	
DIPPMPO/$^{\bullet}SG$	G_2S_2/UV in 0.1 M buffer	*trans*		4.560	1.492	1.421	

able (Fig. 2b), and when the superoxide adduct signal had completely vanished only a weak signal of hydroxyl adduct was observed. However, the formation of DIPPMPO/$^{\bullet}OH$ was almost completely cancelled in the presence of catalase (Fig. 2c). Furthermore, in the presence of methyl alcohol, the hydroxyl adduct signal was suppressed and the $H_2(OH)C^{\bullet}$ radical adduct signal appeared (Fig. 2d). Then, the generation of the hydroxyl adduct during the trapping of superoxide can be attributed to HO$^{\bullet}$ radical trapping rather than to a rearrangement of the superoxide adduct. The presence of HO$^{\bullet}$ radicals could be accounted for, by either decomposition of hydrogen peroxide (resulting from the dismutation of superoxide) or degradation of the superoxide adduct.

A better resolution of the DIPPMPO/$^{\bullet}OOH$ EPR signal was obtained after bubbling N_2 in the solution. As for the DEPMPO/$^{\bullet}OOH$ signal,[9] a dramatic alternate linewidth was observed (Fig. 2e). The spectrum was satisfactorily simulated (Fig. 2f) using the ROKI program,[15] assuming a two site chemical exchange ($k = 19.55 \times 10^6$ s^{-1}) affecting the *trans* diastereoisomer (88%, HOO– *trans* to $(EtO)_2P(O)$–), and the presence of 12% of the *cis* diastereoisomer. The coupling constants (Table 2) calculated for both diastereoisomers are very close to those of DEPMPO/$^{\bullet}OOH$.[9] Our attempts to generate DIPPMPO/$^{\bullet}OOH$ from photolysis of an oxygenated 0.5 mM riboflavin solution in 0.1 M phosphate buffer, in the presence of DETAPAC as an electron donor, resulted in the superimposition (50–50) of the signal of a carbon centred radical adduct ($A_P = 4.68$ mT, $A_N = 1.48$ mT, $A_{H_\beta} = 2.12$ mT) to the DIPPMPO/$^{\bullet}OOH$ signal (Fig. 2g). When SOD (85 u cm^{-3}) was added before photolysis, only the signal of the carbon centred radical adduct was observed.

The superoxide adduct was also detected during photolysis of hydrogen peroxide solutions (10 or 24%) in phosphate buffer. However, the signal of the hydroxyl adduct was superimposed to the DIPPMPO/$^{\bullet}OOH$ signal.

Formation of the DIPPMPO/$^{\bullet}$OOMe adduct. Since alkylperoxyl radicals (ROO$^{\bullet}$) formed during lipid peroxidation play a crucial role in tissue injury, their characterisation in biological milieus is a topic of great interest. Some tertiary alkylperoxyl radicals can be directly detected by EPR at room temperature thanks to their significant lifetimes.[16] Using DMPO the spin trapping technique was only successful in organic milieus.[17] Mason *et al.* reported the trapping of ROO$^{\bullet}$ (R = ^{t}Bu, Me) using DMPO[18] in water. However, they have recently shown that most of the DMPO/$^{\bullet}OOR$ assignments must be reassigned to DMPO/$^{\bullet}OR$.[19] Experiments in our laboratory have already shown that DEPMPO[9,10] is able to trap alkyperoxyl radicals generated either in organic solvents or in water. The resulting spin adducts are persistent and their EPR spectra can be unambiguously assigned.

We investigated the trapping of the methylperoxyl radical ($H_3COO^{\bullet}$) with DIPPMPO. The radical was generated in the presence of the trap by UV-photolysis of an oxygenated H_2O_2 solution in phosphate buffer containing 5% DMSO. The resulting spectrum shown in Fig. 3a was assigned to the DIPPMPO/$^{\bullet}$OOMe adduct not only because of its close similarity to that

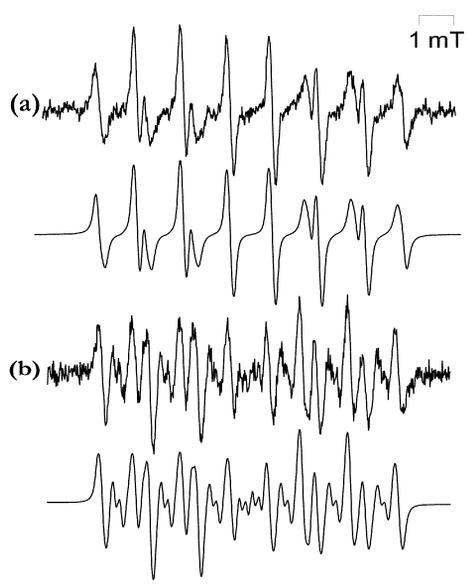

Fig. 3 Observed EPR spectra (a) of the DEPMPO/$^{\bullet}$OOMe spin adduct formed after UV-photolysis of a solution containing 20 mM DIPPMPO, 1% H_2O_2 and 5% DMSO in argon-saturated 0.1 M phosphate buffer at pH 7.4. The curve below is a computer simulation of the signal; (b) of DEPMPO/$^{\bullet}$OMe after a 9-fold dilution in neutral phosphate buffer of the methanolic incubating solution containing 2% MeONa and 0.5 M DIPPMPO. Spectrometer settings: microwave power, 10 mW; modulation amplitude, 0.05 mT; time constant, 0.041 s; gain, 4×10^5; scan range, 20 mT, and scan time, 41 s.

of DIPPMPO/$^{\bullet}$OOH but also because of the insensitivity of its intensity to superoxide dismutase. The DIPPMPO/$^{\bullet}$OOMe spectrum was satisfactorily calculated assuming a two site chemical exchange (k = 21.06 × 10^6 s^{-1}) and the coupling constant values were listed in Table 2. Because of the high oxygen concentration no γ-hydrogen splitting was resolved. As expected in the absence of oxygen, the DIPPMPO/$^{\bullet}$OOMe signal was replaced by the DIPPMPO/$^{\bullet}$Me signal. To confirm our assignment, we generated the DIPPMPO/$^{\bullet}$OMe adduct by nucleophilic addition of MeONa to DIPPMPO in MeOH followed by a nine-fold dilution in neutral phosphate buffer (Fig. 3b). The signal of DIPPMPO/$^{\bullet}$OMe is composed of the signals of the expected *cis* and *trans* diastereoisomers, and obviously its shape prevents misassignment to DIPPMPO/$^{\bullet}$OOMe.

Formation of the DIPPMPO/$^{\bullet}$OH adduct. The very reactive hydroxyl radical seemed often the predominant species contributing to cellular damage. Thus, a good spin trap must offer an unambiguous characterisation of HO$^{\bullet}$ in a biological milieu. Incubation of DIPPMPO with hydrogen peroxide and ferrous sulfate in phosphate buffer (pH = 5.6, 7.0 and 8.3) led to an intense EPR signal (Fig. 4a) composed of a doublet (A_P = 4.688 mT) of quartets (1.2.2.1; A_N = 1.401 mT, A_H = 1.317 mT). It was identical to the signal obtained when DIPPMPO/$^{\bullet}$OOH was submitted to glutathion peroxidase and reduced glutathion. No signal was observed in the presence of catalase. As we mentioned above, the solvated hydroxyl radical was expected to attack DIPPMPO on the side opposite to the diisopropoxyphosphoryl group, and the major signal in Fig. 4a was assigned to the *trans*-DIPPMPO/$^{\bullet}$OH adduct.

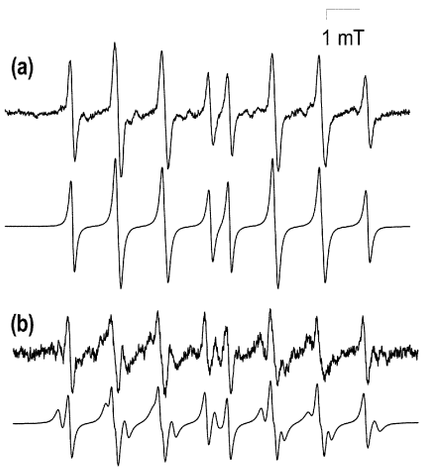

Fig. 4 (a) Observed EPR spectra after hydroxyl radical generation with 2 mM (H_2O_2–$FeSO_4$) system in 0.1 M phosphate buffer at pH 7 in the presence of 0.1 M DIPPMPO (b) and 0.4 M diisopropylmethylphosphonate. Simulation of the spectrum below was made assuming the overlap of the *trans* hydroxyl adduct signal with a carbon centred radical adduct. Spectrometer settings: microwave power, 10 mW; modulation amplitude, 0.005 mT; time constant, 0.041 s; gain, 4 × 10^5; scan range, 15 mT and scan time, 84 s.

In the presence of metal cations, pyrroline *N*-oxides can add water to form the corresponding hydroxylamines which are then oxidised to nitroxides.[20] Nucleophilic addition of water to DMPO in the presence of 0.1 mM ferric ions yields the signal of the DMPO/hydroxyl adduct, however, this signal is inhibited in phosphate buffer or in presence of iron chelators.[5] A solution of DIPPMPO in 100 mM neutral phosphate buffer in the presence of 2 mM $FeNH_4(SO_4)_2$, did not generate DIPPMPO/hydroxyl adduct. In pure water the formation of the DIPPMPO/$^{\bullet}$OH adduct was observed for $FeNH_4(SO_4)_2$ concentrations higher than 0.3 mM.

The signal of the *trans*-DIPPMPO/$^{\bullet}$OH adduct was accompanied by the signal of a very minor adduct (Fig. 4a). Since hydroxyl radicals can easily abstract hydrogen atoms on the α-carbon atoms of an ether, we also addressed the reactivity of the hydroxyl radical towards the DIPPMPO isopropoxyl groups. When the hydroxyl radical was generated in the presence of DIPPMPO and a 4-fold concentration of diisopropylmethylphosphonate [MeP(O)(O^iPr)$_2$], the spectrum shown in Fig. 4b was observed. This spectrum was satisfactorily simulated assuming the presence of the *trans*-DIPPMPO/$^{\bullet}$OH adduct (56%), and of a carbon centred radical adduct (44%, A_N = 1.418 mT, A_P = 4.636 mT, A_{H_β} = 1.933 mT). The latter does not fit with the signal of the minor adduct observed in Fenton experiments, and could correspond to the DIPPMPO/$^{\bullet}$C(Me)$_2$OP(O^iPr)Me adduct.

In the presence of DIPPMPO, UV photolysis (1000 W, Xe–Hg lamp) of a 1% hydrogen peroxide solution in neutral phosphate buffer yielded an intense signal of *trans*-DIPPMPO/$^{\bullet}$OH. Surprisingly the signal intensity continued to increase significantly after the light was shut off. In addition, only a very weak signal of *trans*-DIPPMPO/$^{\bullet}$OH was observed after 1 h storage under day light of a DIPPMPO phosphate buffer solution containing 1% hydrogen peroxide. It has previously been reported that photolysis with a similar UV lamp of DMPO in N_2 saturated neutral phosphate buffer resulted in the formation of DMPO$^{+\bullet}$, which was then hydrolysed to DMPO/$^{\bullet}$OH (eqn. (1), Scheme 3).[21] Hydrated electrons resulting from ionisation of DMPO could react with DMPO to form after protonation DMPO/$^{\bullet}$H which was also observed (eqn. (2), Scheme 3). In the case of DIPPMPO, no DIPPMPO/$^{\bullet}$OH signal was observed when a 0.1 M nitrone solution in neutral phosphate buffer solution also containing 1 mM DTPA was photolysed for 15 min. However, the signal appeared if hydrogen peroxide (1%) was added after the photolysis period. Other authors[22] have suggested that DMPO/$^{\bullet}$OH formed during UV irradiation of DMPO in aqueous solution may arise from the base-catalysed ring opening of an oxaziridine intermediate (eqn. (3), Scheme 3). The diisopropoxyphosphoryl [^{i}PrO)$_2$P(O)] group is a strong electron withdrawing group, and is expected to facilitate hydrolysis of an intermediate oxaziridine to the hydroxylamine. If this hydroxylamine is formed it is then oxidised into DIPPMPO/$^{\bullet}$OH.

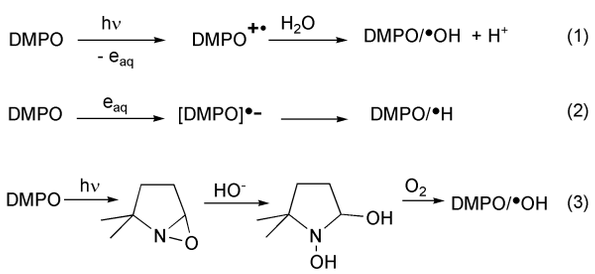

Scheme 3

Formation of DIPPMPO/$^{\bullet}$OR adducts. Alkoxyl adducts DIPPMPO/$^{\bullet}$OR were generated *via* base catalysed nucleophilic addition of the corresponding alcohols to the nitrone, followed by oxidation of the ensuing hydroxylamines. In a typical procedure, a catalytic amount of alcoholate was added to an alcoholic solution of DIPPMPO, and after 30 min of incubation air was bubbled through the solution. The spectra obtained for the methoxyl adduct DIPPMPO/$^{\bullet}$OMe and the *tert*-butyloxyl adduct DIPPMPO/$^{\bullet}$O^{t}Bu are shown in Figs. 3 and 5 respectively, and their EPR parameters are listed in Table 2. As it was already observed with different β-phosphorylated nitrones,[14] the DIPPMPO/$^{\bullet}$OMe signal corresponds to the superimposed spectra of the *cis* and *trans* diastereoisomers. For the *cis*

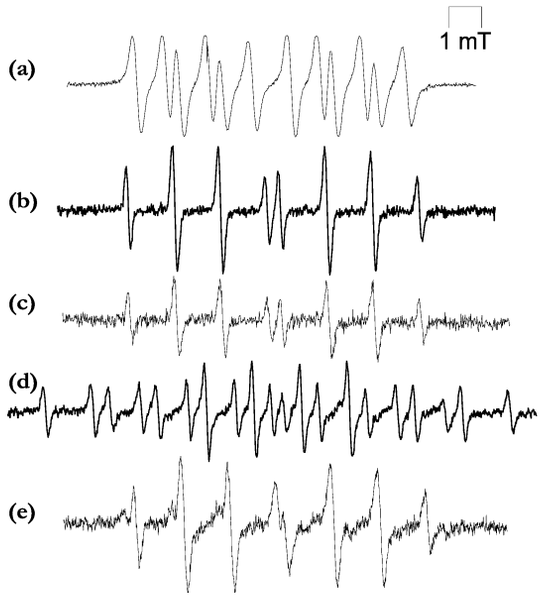

Fig. 5 Observed EPR spectra (a) of DEPMPO/$^{\bullet}$O^{t}Bu in ^{t}BuOH upon incubation of 2% ^{t}BuONa in the presence of 0.5 M DIPPMPO; (b) after 9-fold dilution in neutral phosphate buffer of the (a) incubating solution; (c) after 9-fold dilution in neutral phosphate buffer of a photolysed solution of 10% ^{t}BuOO^{t}Bu in ^{t}BuOH; (d) after 9-fold dilution in neutral phosphate buffer of the ^{t}BuOH incubating solution containing 5% ^{t}BuONa and 0.5 M DIPPMPO; (e) of DEPMPO/$^{\bullet}$SG after photolysis of a 0.1 M neutral phosphate buffer solution containing 0.1 M glutathion disulfide and 0.1 M DIPPMPO. Spectrometer settings: microwave power, 10 mW; modulation amplitude, 0.05 mT; time constant, 0.41 s; gain, (a–d) 6.4×10^5, (e) 8×10^5; scan range, 20 mT and scan time, (a) 41 s, (b)–(e) 84 s.

diastereoisomer, steric repulsion between the methoxyl and diisopropoxyl groups results in the pseudoequatorial position of the C–P bond and thus a smaller phosphorus coupling. For DIPPMPO/$^{\bullet}$O^{t}Bu the spectrum obtained in ^{t}BuOH solution is shown in Fig. 5a. After a ten-fold dilution in phosphate buffer (Fig. 5b), a significant increase of the coupling constant A_{H_β} was observed. DIPPMPO/$^{\bullet}$O^{t}Bu presented in buffer a signal shape close to that of DIPPMPO/$^{\bullet}$OH but their EPR parameters (Table 2) were slightly different. In ^{t}BuOH solution the small A_{H_β} value of DIPPMPO/$^{\bullet}$O^{t}Bu evidences the equatorial position of the C–H$_\beta$ bond, hence, the C–O^{t}Bu bond is axial and is involved in a stabilizing anomeric interaction with the π system of the nitroxyl group. In phosphate buffer, solvation of the nitroxyl group disfavours the anomeric interaction, resulting in the observed increase of A_{H_β} value.

When a too concentrated alcoholate solution was used, the signal of a diphosphorylated nitroxide was observed (Fig. 5d, $A_N = 1.45$ mT, $A_P = 4.93$ mT, $A_P = 4.37$ mT and $A_{H_\beta} = 2.18$ mT).

The DIPPMPO/$^{\bullet}$O^{t}Bu adduct in aqueous phase was also obtained after water dilution of a ^{t}BuOH solution of this adduct obtained after 1 min UV photolysis (using a 1000 W light source) of diterbutylperoxide in the presence of DIPPMPO in ^{t}BuOH (Fig. 5c).

Formation of thiyl centred radical adducts with DIPPMPO. In biological processes, thiyl radicals can be generated from peroxynitrite mediated oxidation of thiols.[23] DMPO is able to trap thiyl radicals in physiologically relevant conditions,[24] however, the glutathiyl spin adduct DMPO/$^{\bullet}$SG is very transient in the presence of peroxynitrite or the superoxide anion.[7b,25] In addition, the DMPO/$^{\bullet}$SG adduct exhibits EPR parameters very close to those of the DMPO/$^{\bullet}$OH adduct,[26] thus making it controversial to discriminate between these two adducts when both $^{\bullet}$SG and HO$^{\bullet}$ are likely to be generated in the presence of DMPO. Using DEPMPO, since the corresponding spin adducts exhibit different phosphorus couplings,[27] it is easier to distinguish between the trapping of $^{\bullet}$SG and that of HO$^{\bullet}$. When a 0.1 M phosphate buffer solution (pH 7.4) containing glutathion disulfide (0.1 M) and DIPPMPO (0.1 M) was irradiated for 1 to 5 min in a quartz cell with a 1000 W Xe–Hg lamp, the spectrum shown in Fig. 5e was observed. As for DEPMPO, even if they have the same pattern (doublet of 1.2.2.1 quartet), the spectra of the DIPPMPO/$^{\bullet}$OH and DIPPMPO/$^{\bullet}$SG adducts can be distinguished owing to slightly different coupling constant values (Table 2).

Formation of carbon centred radical adducts with DIPPMPO. Carbon centred radicals, $^{\bullet}CH_3$, $^{-}{}^{\bullet}CO_2$, $^{\bullet}CH_2OH$ and $^{\bullet}CH(OH)$-CH_3, were generated using a Fenton system in the presence of DMSO, potassium formate, methanol and ethanol, respectively. When these radicals were generated in the presence of DIPPMPO, very intense signals of the corresponding spin adducts were observed. The EPR spectrum of DIPPMPO/$^{\bullet}CO_2K$ can be unambiguously simulated assuming the presence of only one diastereomeric spin adduct. However, for DIPPMPO/$^{\bullet}CH_3$, DIPPMPO/$^{\bullet}CH_2OH$ and DIPPMPO/$^{\bullet}CH(CH_3)OH$, the spectra can be satisfactorily calculated, assuming the presence of either one single diastereoisomer or two diastereoisomers with very close hyperfine coupling constants (Table 2). The formation of two diastereomeric spin adducts for $^{\bullet}CH_3$ and $^{\bullet}CH_2OH$ is in agreement with the formation of two diastereomeric hydroxylamines observed by ^{31}P NMR during the ascorbate reduction of DEPMPO/$^{\bullet}CH_3$ and DEPMPO/$^{\bullet}CH_2OH$.[28] In water, the size of $^{\bullet}CO_2K$ should be dramatically increased by solvation and that could explain the high stereoselectivity of its trapping with either DEPMPO or DIPPMPO.

Kinetic study of the decay of the DIPPMPO/$^{\bullet}$OOH adduct. DIPPMPO/$^{\bullet}$OOH was generated in phosphate buffer (pH = 7.4) using the XO–O_2–HX (0.04 u ml^{-1}: 0.4 mM) system in the presence of DIPPMPO (20 mM). Once the adduct concentration had reached a significant value (after approximately 7 min), the formation of superoxide was quenched by adding a large amount of superoxide dismutase (500 u cm^{-3}). Then, the decay of the adduct was followed by monitoring the intensity of the fourth line of its EPR spectrum (Fig. 6). A simulation of the decay curve using the Daphnis software[29] and assuming a

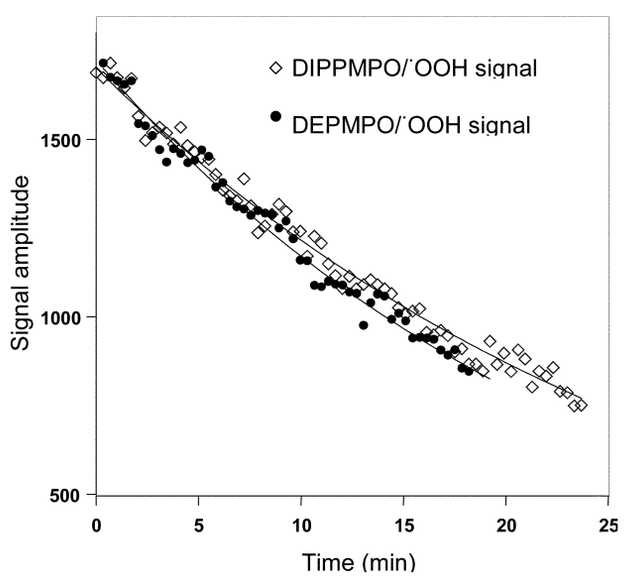

Fig. 6 Observed signal amplitude and simulated EPR decay curves of superoxide adducts when generated in a 0.1 M phosphate buffer solution at pH 7.4 containing 20 mM nitrone, 0.04 u ml^{-1} XO, 0.4 mM HX and 1 mM DTPA, where 500 u ml^{-1} SOD is added after 12 min incubation.

pseudo first order kinetic decay led to a kinetic constant of 53.5×10^{-5} s^{-1}, which corresponds to a half-life of 21 min 36 s. Using the same experimental conditions (the same enzyme batches) a half-life of 18 min was found for DEPMPO/˙OOH ($k_d = 64 \times 10^{-5}$ s^{-1}). The standard deviation between the experimental and calculated curves was in the range of the noise amplitude, except for the first 30 s where a second order dismutation process was likely to occur.

In the presence of SOD, a higher concentration of the DIPPMPO/˙OH adduct was observed during the superoxide decay. When catalase was added to eliminate hydrogen peroxide a significant increase of the DIPPMPO/˙OOH adduct half-life was observed. Hydrogen peroxide or the hydroxyl radical could thus also participate to the decay process of the superoxide adduct. Whatever our experimental conditions, the half-life of DIPPMPO/˙OOH was found 1.2 to 1.4 times higher than that of DEPMPO/˙OOH.

Kinetic study of the decay of the DIPPMPO/˙OH adduct. A Fenton system (2 mM H_2O_2 and 2 mM $FeSO_4$) in phosphate buffer (100 mM) at pH 7 in the presence of DEPMPO or DIPPMPO (0.05 M) was used to obtain the corresponding hydroxyl adducts. Afterwards, catalase (650 u cm^{-3}) was added to quench the radical generating system and the decay of the signal amplitude was monitored by EPR (Fig. 7). The decay

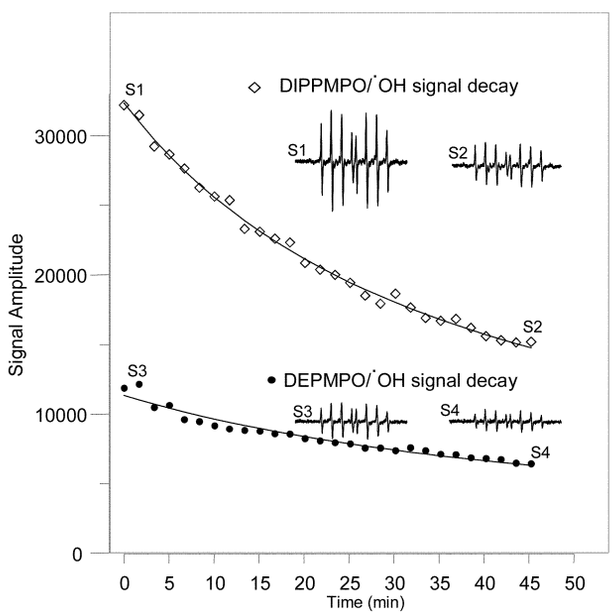

Fig. 7 Observed signal amplitude and simulated EPR decay curves of hydroxyl adducts when generated in a 0.1 M phosphate buffer solution at pH 7.4 containing 50 mM nitrone, 2 mM ferrous sulfate and 2 mM hydroperoxide,where 650 u ml^{-1} catalase is added after 7 min incubation.

curves were satisfactory simulated assuming a second order decay process and for each adduct the half life was estimated as the inverse ratio of the product of the decay rate constant (k_d = 7.87 M^{-1} s^{-1} for DEPMPO/˙OH and k_d = 7.46 M^{-1} s^{-1} for DIPPMPO/˙OH) by the initial adduct concentration. Initial concentration values ([DEPMPO/˙OH] = 3.72×10^{-5} M, [DIPPMPO/˙OH] = 5.85×10^{-5} M) were obtained using a calibration curve established from TEMPO solutions. With the above k_d values and concentrations, the estimated half-life was 38 min for DIPPMPO/˙OH and 57 min for DEPMPO/˙OH. This study shows that the DIPPMPO/˙OH adduct is slightly more persistent than the DEPMPO analogue. DIPPMPO/˙OH is likely enough persistent to reach and maintain an important concentration inducing disproportionation as the main decay process.

Conclusion

DIPPMPO is an analogue of DEPMPO, easy to prepare and easy to purify. DIPPMPO is more lipophilic than DEPMPO and could thus be more appropriate to trap radicals in lipophilic environments. In phosphate buffer, DIPPMPO is as efficient as DEPMPO to trap various free radicals, and its superoxide and hydroxyl adducts are slightly more persistent than those of DEPMPO. The superoxide adduct decays with a pseudo first order kinetics, while the hydroxyl adduct decays with second order kinetics. DIPPMPO/˙OH is significantly more persistent than the superoxide adduct, and thus its disproportionation is likely the main decay process of DIPPMPO/˙OH but not of DIPPMPO/˙OOH.

Experimental

Chemicals

Drying of the solvents was made by distillation under inert atmosphere in the presence of sodium and benzophenone for THF and toluene, or magnesium for methanol, ethanol and ethoxyethanol. Melting points were taken on a Büchi capillary apparatus and were left uncorrected. NMR spectra were obtained on Brucker AC 100 (^{31}P NMR 40.5 MHz), Brucker AC 200 (^{1}H NMR 200 MHz and ^{13}C NMR 50.3 MHz), and Bruker AM 400 X (^{1}H NMR 400 MHz and ^{13}C NMR 100.6 MHz) spectrometers. Chemical shifts are reported as δ values relative to internal and external tetramethylsilane for ^{1}H and ^{13}C NMR respectively, and to external 85 wt.% phosphoric acid for ^{31}P NMR. The interpretation of the spectra was achieved by comparing heteronuclear ^{13}C–^{1}H chemical shift correlation and ^{1}H homonuclear correlation (*cf.* Fig. 1 for numbering). Mass spectra were recorded in the FAB^+ or $LSIMS^+$ mode on a ZabSpec TOF Micromass spectrometer.

Diisopropyl (2-methyl-2-pyrrolidinyl)phosphonate. 2-Methylpyrroline was purchased from Sigma-Aldrich chemical company and was 95% pure. It was distilled before use on 4 Å molecular sieves at 30 °C under 16 mm Hg pressure. This product 15.8 g, *ca.* 0.190 mol was added at 20 °C to 32 cm^3 (0.193 mol) of diisopropylphosphite (98% pure from Strem Chemicals Inc.). The reaction mixture was stirred in the dark for several days (12 days) at 20–30 °C under inert atmosphere and then 0.2 eq. (6.4 ml) of diisopropylphosphite were added to complete the reaction. When 2-methylpyrroline was no longer detectable by TLC, 100 cm^3 of 2 M HCl were added and the aqueous phase was washed twice with 50 cm^3 of CH_2Cl_2. After adjustment of the pH to 9 by addition of Na_2CO_3, the aqueous phase was extracted 3 times with CH_2Cl_2. The organic phase was dried on $MgSO_4$ and 39.83 g of an orange oil corresponding to diisopropyl (2-methyl-2-pyrrolidinyl)phosphonate (84 % yield) was obtained after solvent evaporation. The product purity was verified through NMR and CPG studies. Found: C, 52.98; H, 9.75; N, 5.60. $C_{11}H_{24}NO_3P$ requires C, 52.99; H, 9.70; N, 5.62%. δ_P (40.5 MHz; $CDCl_3$; H_3PO_4) 28.28. δ_H (100.13 MHz; $CDCl_3$; Me_4Si) 4.5–4.9 (2H, m, $OCHMe_2$), 2.9–3.1 (2H, m, CH_2N), 2.4–1.5 (4H, m, CH_2), 1.329 (3H, d, $J_{H,H}$ 6.21, CH_3), 1.317 (3H, d, $J_{H,P}$ 15.28, CH_3), 1.307 (3H, d, $J_{H,H}$ 6.13, CH_3). δ_C (50.32 MHz; $CDCl_3$; Me_4Si), 70.46 (1C, d, $J_{C,P}$ 8.05, $OCHMe_2$), 70.3 (1C, d, $J_{C,P}$ 8.92, $OCHMe_2$), 59.4 (1C, d, $J_{C,P}$ 165.4, NCMeP), 47.1 (1C, d, $J_{C,P}$ 8.3, CH_2), 34.54 (1C, d, $J_{C,P}$ 2.5, CH_2), 25.75 (1C, d, $J_{C,P}$ 5.53, CH_2), 24.4, 24.3, 24.2 and 24.0 (4C, CH_3) 24.0 (1C, d, $J_{C,P}$ 6.2, CH_3).

5-Diisopropoxyphosphoryl-5-methyl-1-pyrroline *N*-oxide. Diisopropyl (2-methyl-2-pyrrolidinyl)phosphonate (42.87 g, 0.172 mol) was added to 2.032 g (0.007 mol) of sodium tungstate dissolved in 100 cm^3 of distilled water. To the solution cooled down to 0 °C, 35.35 cm^3 (0.378 mol) of 35 % H_2O_2 were

added dropwise. The pale yellow reaction mixture was stirred at 0 °C until the colour darkened, then it was stirred at 6 to 10 °C for several hours, and the progress of the oxidation was monitored by TLC. When the oxidation stopped, a new quantity of H_2O_2 (8 cm^3, 0.5 eq.) was added to oxidise the pyrrolidinyl residue. When the reaction was virtually complete the expected nitrone was extracted with 8 times 100 cm^3 of CH_2Cl_2. The collected organic phase was dried with $MgSO_4$ and the solvent was removed under reduced pressure. The crude nitrone (43.35 g) was crystallised at −18 °C under inert and dry atmosphere. Once the nitrone was crystallised, dry pentane and toluene (90:10) were added under argon atmosphere at room temperature until crystals were dissolved. The pure product was then quickly filtered under argon flush. Successive crystallisations and recrystallisations allowed us to collect 30 g of DIPPMPO (66% yield PM = 263.276) in the form of very hydrophilic yellow plate crystals, melting with room wetness. These crystals suitable for X ray investigation were stored under argon at −18 °C. Found : C, 46.82; H, 8.48; N, 4.43. $C_{11}H_{22}NO_4P$ requires C, 50.18; H, 8.42; N, 5.32% but [$C_{11}H_{22}NO_4P$ + 1 H_2O] requires C, 46.88; H, 8.58; N, 4.97% (measurements were not made in dry atmosphere). δ_P (40.5 MHz; $CDCl_3$; H_3PO_4) 19.74. δ_H (400.13 MHz; $CDCl_3$; Me_4Si) 6.822 (1H, q, $J_{H,P}$ 2.8, $J_{H,H}$ 2.8, HC=N), 4.81 (1H, d sept., $J_{H,P}$ 0.6, $J_{H,H}$ 6.3, $OCHMe_2$), 4.72 (1H, d sept., $J_{H,P}$ 1.1, $J_{H,H}$ 6.3, $OCHMe_2$), 2.65–2.81 (2H, m, CH_2), 2.44–2.55 (1H, m, CH_2–), 1.92–2.08 (1H, m, CH_2), 1.60 (3H, d, $J_{H,H}$ 14.79, CH_3), 1.306 (3H, dd, $J_{H,P}$ 0.24, $J_{H,H}$ 6.3, CH_3), 1.286 (3H, d, $J_{H,H}$ 6.3, CH_3), 1.282 (3H, d, $J_{H,H}$ 6.3, CH_3), 1.277 (3H, d, $J_{H,H}$ 6.3, CH_3). δ_C (100.6 MHz; $CDCl_3$; Me_4Si) 134.55 (1C, d, $J_{C,P}$ 8.05, –HC=N), 75.15 (1C, d, $J_{C,P}$ 157.94, NCMeP), 72.79 (1C, d, $J_{C,P}$ 7.04, $OCHMe_2$), 71.54 (1C, d, $J_{C,P}$ 7.01, $OCHMe_2$), 31.18 (1C, s, CH_2), 25.83 (1C, s, CH_2), 24.55 (1C, d, $J_{C,P}$ 1.71, CH_3), 24.16 (1C, d, $J_{C,P}$ 3.82, CH_3), 23.99 (1C, d, $J_{C,P}$ 5.13, CH_3), 23.7 (1C, d, $J_{C,P}$ 6.74, CH_3), 21.03 (1C, s, CH_3).

X-ray crystallographic determinations

A crystal mounted in inert oil on a glass fiber was transferred to the cold gas stream of the diffractometer. The approximate dimensions of this crystal were (0.6 × 0.4 × 0.3 mm).

Crystal data ‡

$C_{11}H_{22}NO_4P$, M = 263.27, monoclinic symmetry cell setting, unit-cell dimensions a =14.4667(4) Å, b = 8.2687(3) Å, c = 12.4192(5) Å, cell volume V = 1485.32(9) Å^3, cell measurement temperature = 293(2) K, symmetry space group name H–M $P2_1/c$, cell formula units Z = 4, data collection with CAD 4-diffractomer radiation of Mo Kα type, absorption coefficient μ = 1.88 mm^{-1}, 3122 cell reflections measured. 2978 unique reflections with equivalent R = 0.045 which were used in all calculations. The final wR factor was 0.1285 (all data). The data were collected according to the reference manual Kappa CCD (Nonius, 1998).[30] The cell refinement and the data reduction were performed by 'Denzo and Scalepak (Otwinowski and Minor, 1997)' computing.[31] The structure resolution computing was SIR (Altamore, 1994).[32] The structure refinement and the audit creation method were performed using the SHELXL-97 program.[33]

Determination of the octanol–aqueous solution partition coefficient (K_p)

UV spectra were recorded using a computer controlled UNICAM UV/visible UV4 spectrometer. Solutions of DIPPMPO were prepared in water or 0.1 M phosphate buffer at various concentrations (2 to 20 mM) and their optical absorption maxima were measured for λ_{max} = 269 nm. From these values an absorbency calibration curve was plotted as a function of concentration. Only the linear part of the curve was used for the further determination of the DIPPMPO concentration. Then 2 cm^3 of octanol were mixed with an equal volume of 20 mM DIPPMPO solution either at 25 °C for water solution or at 37 °C for 0.01 M phosphate buffer solution. The mixture was vigorously stirred for 1 h and the aqueous and octanolic phases were separated by brief centrifugation (3500*g* for 60 s). The partition coefficient was measured as the ratio of the DIPPMPO concentration in octan-1-ol to that in water or buffer.

Spin-trapping studies

Xanthine oxidase (from cow milk, phosphate free) and superoxide dismutase (from bovine erythrocyte) were obtained from Bœringer Mannheim Biochemica Co. Catalase (from bovine liver, 2000–5000 u mg^{-1}), glutathione peroxidase (from bovine erythrocyte) and all chemicals were purchased from Sigma Chemical Co. Distilled water for the aqueous solution or buffers was stirred before use for 6 h in the presence of a sodium iminodiacetate chelating resin (4×10^{-2} g cm^{-3}) to remove trace metal impurities. EPR spectra were mainly recorded at room temperature on a Bruker ESP 300 EPR spectrometer at 9.5 GHz (X-band) using 100 kHz field modulation and equipped with a NMR gaussmeter for magnetic field calibration. An HP 5350B microwave frequency counter was used for the determination of Landé factors g. EPR assays with riboflavin were carried out using a computer-controlled Varian E-9 EPR spectrometer operating at the X-band with 100 KHz modulation frequency. EPR spectra of peroxyl radicals were simulated using a computer simulation program ROKI.[15]

Spin-trapping of superoxide generated by the (xanthine oxidase–oxygen–hypoxanthine) system. The $O_2^{-\bullet}$ radicals were generated by HX (0.4 mM), and XO (0.4 or 0.04 u cm^{-3}) in the presence of nitrone (0.1 or 0.05 or 0.02 M) and DETAPAC (1 mM), in phosphate buffer (0.1 M) at various pH (5.6, 7 and 8.2). The first EPR recording was performed 60 s after enzyme addition. When necessary, the superoxide adduct formation was inhibited by addition of 200–500 u $cm^{-3}$of SOD to the reaction mixture.

Spin-trapping of superoxide generated by the (riboflavin–visible light–oxygen) system. The $O_2^{-\bullet}$ radicals were generated by photolysis of a solution of riboflavin (0.5 mM) and DETAPAC (1 mM) in phosphate buffer 0.1 M containing also the nitrone (0.1 M). Photolysis was performed either outside or directly inside the spectrometer cavity using a quartz cell and a tungsten filament 100 W Krypton lamp or a 430 nm blue LED lamp as the visible light source. The first EPR recording was performed 1 min after photolysis started.

Spin-trapping of the hydroxyl radical generated by a Fenton system. A Fenton system including H_2O_2 (2 mM), DETAPAC or EDTA (1 mM) and $FeSO_4$ (2 mM) in phosphate buffer (100 mM) was used in the presence of nitrone (0.02 M to 0.1 M). The first spectra of each experiment series were recorded 1 min after addition of the last reagent ($FeSO_4$). To inhibit the formation of the hydroxyl adduct 650 u cm^{-3} catalase was added before $FeSO_4$. For the kinetic studies of the decay of the hydroxyl adduct, catalase was added 7 min after $FeSO_4$.

Spin-trapping of the hydroxyl radical generated by H_2O_2 photolysis. A solution in phosphate buffer (100 mM) of either 1% or 10 % or 24 % H_2O_2, containing also 1 mM DTPA and 0.1 M nitrone was photolysed during 3 min with a 1000 W xenon–

‡ CCDC reference number 190377. See http://www.rsc.org/suppdata/p2/b2/b206909c/ for crystallographic files in .cif or other electronic format.

mercury Oriel lamp. The first spectra of each experiment series were recorded instantaneously after photolysis.

Spin-trapping of the methylperoxyl radical generated by DMSO–H_2O_2 photolysis. MeOO$^{\bullet}$ was produced by 2 min UV-photolysis (with a 1000 W xenon–mercury Oriel lamp) of an oxygen-saturated phosphate buffer solution (0.1 M, pH 7.4) containing H_2O_2 (1% v/v), DMSO (5 %) and DIPPMPO (20 mM).

DIPPMPO/$^{\bullet}$OMe adduct generation. 5% $Pb(OAc)_4$ or 2% CH_3ONa was added to a methanolic solution of 0.5 M DIPPMPO. After 30 min, 10 µl of the solution were added to 90 µl of phosphate buffer (0.1 M, pH 7.4).

DIPPMPO/$^{\bullet}$O^{t}Bu adduct generation. 2% ^{t}BuONa was added to a ^{t}BuOH solution of 0.5 M DIPPMPO. After 30 min, 10 µl of the solution were added to 95 µl of phosphate buffer (0.1 M, pH 7.4). Another procedure consisted in photolysing for 1 min 10% ^{t}BuOO^{t}Bu in a ^{t}BuOH solution of 0.5 M DIPPMPO and adding 10 µl of this solution to 90 µl of phosphate buffer (0.1 M, pH 7.4).

Spin-trapping of carbon centred radicals generated by action of the hydroxyl radical on alcohol or DMSO. The HO$^{\bullet}$ radical was generated either by a Fenton system or the photolysis of hydrogen peroxide in the presence of nitrone (0.1 M) and alcohol (10%) or 200 mM DMSO. The first spectrum of each experiment series was recorded 1 min after reagent mixing.

Spin-trapping of the glutathionyl radical GS$^{\bullet}$ generated by UV-photolysis of glutathion disulfide. The spectra were recorded after 1 min to 5 min photolysis (using a 600 W xenon–mercury arc) of a phosphate buffer solution (0.1 M, pH 7.4) containing 0.1 M GSSG and the nitrone (0.1 M) in a quartz cell.

References

1 M. C. R. Symons, *Chemical and Biochemical Aspects of Electron Spin Resonance*, Van Nostrand-Reinhold, New York, 1978, 190.

2 (*a*) P. J. Thornalley, *Life Chem. Rep.*, 1986, **4**, 57–112; (*b*) E. Finkelstein, G. M. Rosen and E. J. Rauckman, *Arch. Biochem. Biophys.*, 1980, **200**, 1–16; (*c*) G. M. Rosen and E. Finkelstein, *Adv. Free Radical Biol. Med.*, 1985, **1**, 345–375.

3 J. A. DeGray and R. P. Mason, *Biological Spin Trapping*, in *Electron Spin Resonance*, ed. N. M. Atherton, M. J. Davies and B. C. Gilbert, Royal Society of Chemistry, Cambridge, UK, 1994, vol. 14, pp. 246–301.

4 (*a*) M. C. Krishna, D. A. Grahame, A. Samuni, J. B. Mitchell and A. Russo, *Proc. Natl. Acad. Sci. USA*, 1992, **89**, 5537–5541; (*b*) M. C. Krishna, A. Russo, J. B. Mitchell, S. Goldstein, H. Dafni and A. Samuni, *J. Biol. Chem.*, 1996, **271**, 26026–26031.

5 (*a*) A. R. Forrester and S. P. Hepburn, *J. Chem. Soc. (C)*, 1971, 701–703; (*b*) M. J. Davies, B. C. Gilbert, J. K. Stell and A. C. Whitwood, *J. Chem. Soc., Perkin Trans. 2*, 1992, 333–335.

6 P. M. Hanna, W. Chamulitrat and R. P. Mason, *Arch. Biochem. Biophys.*, 1992, **296**, 640–644.

7 (*a*) E. Finkelstein, G. M. Rosen, E. J. Rauckman and J. Paxton, *Mol. Pharmacol.*, 1979, **16**, 676–685; (*b*) G. R. Buettner, *Free Radical Res. Commun.*, 1993, **19**, 579–587.

8 (*a*) E. Finkelstein, G. M. Rosen and E. J. Rauckman, *J. Am. Chem. Soc.*, 1980, **102**, 4994–4999; (*b*) A. Samuni, C. Murali Krishna, P. Riesz, E. Finkelstein and A. Russo, *Free Radical Biol. Med.*, 1989, **6**, 141–148; (*c*) G. R. Buettner, *Free Radical Res. Commun.*, 1990, **10**, 11–15.

9 (*a*) C. Frejaville, H. Karoui, B. Tuccio, F. Le Moigne, M. Culcasi, S. Pietri, R. Lauricella and P. Tordo, *J. Med. Chem.*, 1995, **38**, 258–265; (*b*) S. Barbati, J. L. Clément, G. Olive, V. Roubaud, B. Tuccio and P. Tordo, *Free Radicals in Biology, Environment*, ed. F. Minisci, NATO ASI Series, Life Sciences, Kluwer Academic Publishers, Dordrecht, The Netherlands, 1997, ch. 3, pp. 39–47.

10 H. Karoui, F. Chalier and P. Tordo, to be published.

11 S. Barbati, J. L. Clément, C. Frejaville, J. C. Bouteiller, P. Tordo, J. C. Michel and J. C. Yadan, *Synthesis*, 1999, **12**, 2036–2040.

12 K. Stolze, N. Udilova and H. Nohl, *Free Radical Biol. Med.*, 2000, **29**, 1005–1014.

13 (*a*) E. A. Konorev, J. E. Baker, J. Joseph and B. Kalyanaraman, *Free Radical Biol. Med.*, 1993, **14**, 127; (*b*) E. G. Janzen, J. L. Poyer, C. F. Schaefer, P. E. Downs and C. M. Dubose, *J. Biochem. Biophys. Methods*, 1995, **30**, 239.

14 (*a*) B. Halliwell, *Am. J. Med.*, 1991, **91**(3C), 14S–22S; (*b*) B. Halliwell and J. M. C. Gutteridge, *Am. J. Med.*, 1984, **219**, 1–14; (*c*) B. Halliwell and S. Chirico, *Am. J. Clin. Nutr.*, 1993, **57(S)**, 715S–725S.

15 A. Rockenbauer and L. Korecz, *Appl. Magn. Reson.*, 1996, **10**, 29–48.

16 B. Kalyanaraman, C. Mottley and R. P. Mason, *J. Biol. Chem.*, 1983, **258**, 3855–3858.

17 (*a*) M. J. Davies and T. F. Slater, *Biochem. J.*, 1986, **240**, 789–795; (*b*) E. G. Janzen, P. H. Krygsman, D. A. Lindsay and D. L. Haire, *J. Am. Chem. Soc.*, 1990, **112**, 8279–8284; (*c*) W. Bors, C. C. Michel and K. Stettmaier, *J. Chem. Soc., Perkin Trans. 2*, 1992, 1513–1517.

18 W. Chamulitrat, N. Takahashi and R. P. Mason, *J. Biol. Chem.*, 1989, **264**, 7889–7899.

19 S. I. Dikalov and R. P. Mason, *Free Radical Biol. Med.*, 1999, 864–872.

20 K. B. G. Torssell, *Nitrile Oxides, Nitrones and Nitronate in Organic Synthesis*, in *Organic Nitrochemistry Series*, ed. H. Feuer, VCH publishers, Inc, New York, 1988, pp. 75–93.

21 C. F. Chignell., A. G. Motten, R. H. Sik, C. E. Parker and K. Reszka, *Photochem. Photobiol.*, 1994, **59**, 5–11.

22 M. J. Davies, L. G. Forni and S. L. Shuter, *Chem. Biol. Interact.*, 1987, **61**, 177–188.

23 R. Radi, J. S. Beckman, K. M. Bush and B. A. Freeman, *Arch. Biochem. Biophys.*, 1991, **288**, 481–487.

24 (*a*) L. S. Harman, D. K. Carver, J. Schreiber and R. P. Mason, *J. Biol. Chem.*, 1986, **261**, 1642–1648; (*b*) O. Augusto, R. M. Gatti and R. Radi, *Arch. Biochem. Biophys.*, 1994, **310**, 118–125; (*c*) J.-N. Lemercier, G. L. Squadrito and W. A. Pryor, *Arch. Biochem. Biophys.*, 1995, **321**, 31–59; (*d*) S. Pou, S. Y. Nguyen, T. Gladwell and J. M. Rosen, *Biochem. Biophys. Acta*, 1995, **1244**, 62–68.

25 H. Karoui, N. Hogg, J. Joseph and B. Kalyanaraman, *Arch. Biochem. Biophys.*, 1996, **330**, 115–124.

26 B. Kalyanaraman, H. Karoui, R. J. Singh and C. C. Felix, *Anal. Biochem.*, 1996, **241**, 75–81.

27 H. Karoui, N. Hogg, C. Fréjaville, P. Tordo and B. Kalyanaraman, *J. Biol. Chem.*, 1996, **271**, 6000–6009.

28 V. Kramtsov, L. J. Berliner and T. L. Clanton, *Magn. Res. Med*, 1999, **42**, 228–234.

29 R. Lauricella, *Daphnis program*, Université de Provence, Marseille, France, 1997.

30 B. V. Nonius Kappa CCD Reference Manual., P.O Box 811, 2600 Av. Delft, The Netherlands, 1998.

31 Z. Otwinowski and W. Minor, in *Processing of X-ray Diffraction Data Collected in Oscillation Mode*, *Methods in Enzymology, Vol. 276: Macromolecular Crystallography*, ed. C. W. Carter, Jr and R. M. Sweet, Academic Press, 1997, part A, pp. 307–326.

32 A. Altamore, G. Cascarano, C. Giacovazzo, A. Guagliardi, M. C. Burla, G. Polidori and M. Camalli, *J. Appl. Cryst.*, 1994, **27**, 435–436.

33 G. M. Sheldrick, *SHELXL-97*, *Program for the Refinement of Crystal Structures*, University of Gëottingen, Germany, 1997.